Available online at www.sciencedirect.com
SCIENCE DIRECT
Journal of Non-Crystalline Solids 352 (2006) 3326–3331
JOURNAL OF NON-CRYSTALLINE SOLIDS
www.elsevier.com/locate/jnoncrysol

Structural and magnetic investigations of Fe_2O_3–TeO_2 glasses

A. Mekki [a], G.D. Khattak [a], L.E. Wenger [b,*]

[a] Department of Physics, King Fahd University of Petroleum and Minerals, Dhahran 31261, Saudi Arabia
[b] Department of Physics, The University of Alabama at Birmingham, Birmingham, AL 35294-1170, USA

Received 26 September 2005
Available online 22 June 2006

Abstract

A series of tellurite glasses containing Fe_2O_3 with the nominal composition $x(Fe_2O_3)$–$(1-x)(TeO_2)$, where $x = 0.05$, 0.10, 0.15, and 0.20, have been synthesized and investigated using X-ray photoelectron spectroscopy (XPS) and magnetization techniques. The Te 3d core level spectra for all glass samples show symmetrical peaks at essentially the same binding energies as measured for TeO_2 indicating that the chemical environment of the Te atoms in these glasses does not vary significantly with the addition of Fe_2O_3. Furthermore, the full-width at half-maximum (FWHM) of each peak does not vary with increasing Fe_2O_3 content which suggests that the Te ions exist in a single configuration, namely TeO_4 trigonal bipyramid (tbp). The O 1s spectra are narrow and symmetric for all compositions such that oxygen atoms in the Te–O–Te, Fe–O–Fe and Te–O–Fe configurations must have similar binding energies. The analysis of the Fe 3p spectra indicates the presence of Fe^{3+} ions only, which is consistent with the valence state of the Fe ions determined from magnetic susceptibility measurements.

PACS: 61.14.Qp; 61.43.Fs; 75.20.−g

Keywords: Magnetic properties; Tellurites; Structure

1. Introduction

Tellurium oxide (TeO_2) based glasses are important in the fields of glass science and technology due to their electrical and optical properties. TeO_2 is of particular importance as this conditional glass network former has a low melting point when combined with an alkali metal oxide or a transition metal (TM) oxide [1,2]. The formation of these glasses may also be accompanied by a change in the local TeO_2 structure. For example, the addition of alkali metal ions in tellurite glasses can result in the transformation of some TeO_4 trigonal bipyramid (tbp) structural units into TeO_3 trigonal pyramid (tp) with non-bridging oxygen [3]. Similar transformations of the TeO_4 structural unit into the TeO_3 tp structure were found with increasing V_2O_5 content in V_2O_5–TeO_2 glasses and with increasing WO_3 content in WO_3–TeO_2 glasses [4,5]. However, our recent studies on CuO- and MoO_3-tellurite glasses [6,7] detected no TeO_3 structural units in the XPS spectra, although the existence of both TeO_4 and TeO_3 structural units were found in the ternary Fe_2O_3–Na_2O–TeO_2 glass system [8]. Thus studies of the tellurite glass structure and its corresponding effect on the electronic properties continue to be investigated by a multitude of techniques.

Several spectroscopic techniques have been used to investigate the structure of tellurite glasses, including IR [9], Raman [10], NMR [11], X-ray absorption [12] and neutron diffraction [13]. Similarly, X-ray photoelectron spectroscopy (XPS) is a powerful technique for studying the local glass structure as a function of the TM oxide concentration as well as distinguishing between bridging oxygen (BO) and non-bridging oxygen (NBO) [14]. In the present study the effect of Fe_2O_3 on the local glass structure in the tellurite glass system is investigated by XPS, and is

* Corresponding author. Tel.: +1 205 934 5102; fax: +1 205 975 6111.
E-mail address: wenger@uab.edu (L.E. Wenger).

0022-3093/$ - see front matter © 2006 Elsevier B.V. All rights reserved.
doi:10.1016/j.jnoncrysol.2006.05.007

part of our continuing studies of the glass structure in transition metal-doped tellurite glasses [6–8]. Besides checking on the whether any TeO_4 units transform into TeO_3 units at high Fe_2O_3 content, the oxidation state of the Fe ions can be deduced from the XPS spectra. Temperature-dependent magnetic susceptibility measurements in combination with inductively coupled plasma spectroscopy (ICP) provide an independent measure of the Fe valence state in these glasses as well as characterize the nature of the magnetic interactions between the Fe ions.

2. Experimental details

2.1. Sample preparation

All glasses were prepared by melting dry mixtures of reagent grade Fe_2O_3 and TeO_2 in alumina crucibles to form nominal $x(Fe_2O_3)$–$(1-x)(TeO_2)$ compositions with $x = 0.05$, 0.10, 0.15, and 0.20. Since oxidation and reduction reactions in a glass melt are known to depend on the size of the melt, on the sample geometry, on whether the melt is static or stirred, on thermal history, and on quenching rate, all glass samples were prepared under similar conditions to minimize these factors. Approximately 30 g of chemicals were thoroughly mixed in an alumina crucible to obtain a homogenized mixture for each Fe_2O_3 concentration. The crucible containing the nominal mixture was then transferred to an electrically heated melting furnace maintained at 900–1000 °C. The melt was left for about an hour under atmospheric conditions in the furnace during which the melt was occasionally stirred with an alumina rod. The homogenized melt was then cast onto a stainless steel plate mold to form glass rods of approximately 5-mm diameter and 2 cm in length for XPS measurements. After casting, the specimens were annealed at 200 °C for ten hours and stored in a vacuum desiccator to minimize any further oxidation of the glass samples. The actual compositions of the glasses were determined by inductively coupled plasma spectroscopy (ICP) and are presented in Table 1. Although the inclusion of alumina from the crucibles used in the melting of the glass mixtures can be a possible source of impurities, no signals for aluminum were detected in either the XPS or ICP measurements on these glasses. X-ray diffraction performed on the samples confirmed the amorphous nature of these glasses.

Table 1
Nominal and actual composition (molar fraction) of various tellurite glasses containing Fe_2O_3

Nominal		Actual (from ICP)	
Fe_2O_3	TeO_2	Fe_2O_3	TeO_2
0.05	0.95	0.046	0.954
0.10	0.90	0.089	0.911
0.15	0.85	0.135	0.865
0.20	0.80	0.153	0.847

The relative uncertainty in the ICP results is ±5%.

2.2. XPS measurements

Core level photoelectron spectra were collected on a VG scientific ESCALAB MKII spectrometer equipped with a dual aluminum–magnesium anode X-ray gun and a 150-mm concentric hemispherical analyzer using Al $K\alpha$ ($h\nu = 1486.6$ eV) radiation from an anode operated at 130 W. Photoelectron spectra of Te 3d, Fe 2p, Fe 3p, and O 1s core levels were recorded using a computer-controlled data acquisition system with the electron analyzer set at a pass-energy of 20 eV for the high resolution scans. For self-consistency, the C 1s transition at 284.6 eV was used as a reference for all charge shift corrections. This peak arises from hydrocarbon contamination and its binding energy is generally accepted as remaining constant, irrespective of the chemical state of the sample. For XPS measurements, a glass rod from each composition was cleaved in the preparation chamber at a base pressure of 2×10^{-9} mbar before being transferred to the analysis chamber where the pressure was maintained at $\sim 2 \times 10^{-10}$ mbar. A non-linear, least-squares algorithm was employed to determine the best fit to each of the O 1s, Fe 3p, and Te 3d spin–orbit doublet spectra with two Gaussian–Lorentzian curves in order to represent bridging and non-bridging oxygen, the two possible Fe oxidation states (Fe^{3+} and Fe^{2+}), and the two possible Te tbp and tp structural units, respectively. The fractions of non-bridging oxygen, Fe^{3+}, and tbp units were determined from the respective area ratios obtained from these fits. Based on the reproducibility of similar quantitative spectral decompositions of spectra taken from other surfaces on the same glass samples, uncertainties of ±5% for NBO content and ±10% for both Fe^{3+} and TeO_4 units were estimated for these area ratios. A period of approximately 2 h was required to collect the data set for each sample.

2.3. Magnetic measurements

The temperature-dependent DC magnetic susceptibility was measured using a SQUID magnetometer (Quantum Design model MPMS-5S) in a magnetic field of 5000 Oe over a temperature range 5–300 K at temperature intervals of 2.5 K. The susceptibility of the sample holder was negligible for all samples, and the overall accuracy of the magnetic measurements is estimated to be approximately 3% due to the uncertainty of the magnetometer calibration.

3. Results

3.1. Te 3d spectra

Fig. 1 displays the Te 3d spin–orbit core level spectra for all glass samples investigated. It is clear from the figure that the peak intensity decreases with increasing Fe_2O_3 content, while the peak positions remain essentially the same for all glass compositions. The binding energies (BE) of the $Te\,3d_{5/2}$ are measured to be 576.2 ± 0.1 eV with a

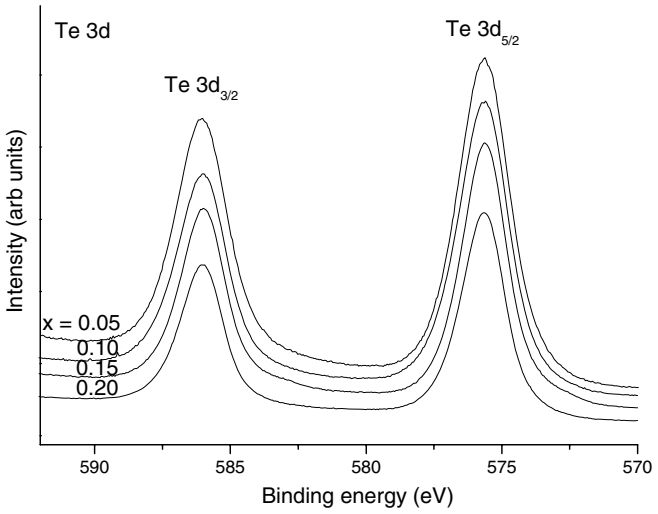

Fig. 1. Core level Te 3d spectra for the $x(Fe_2O_3)$–$(1-x)(TeO_2)$ glasses.

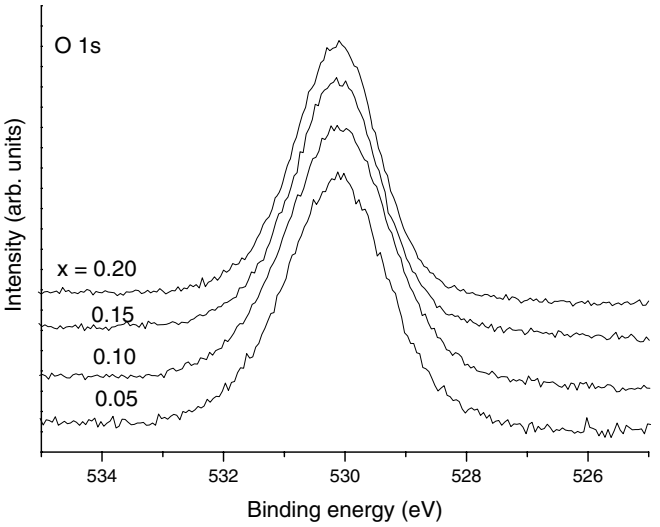

Fig. 2. Core level O 1s spectra for the $x(Fe_2O_3)$–$(1-x)(TeO_2)$ glasses.

Table 2
Peak positions in eV for the core levels Te $3d_{5/2}$, Fe $2p_{3/2}$, Fe 3p, and O 1s relative to C 1s (284.6 eV) and their corresponding FWHM (full-width at half-maximum)

x	Te $3d_{5/2}$ FWHM	ΔE Te3d	Fe $2p_{3/2}$ FWHM	ΔE Fe2p	Fe 3p FWHM	O 1s
0.05	576.2	10.4	710.8	14.0	55.9	530.2
	2.3				3.1	2.1
0.10	576.3	10.4	710.8	14.0	55.9	530.1
	2.2				3.2	2.1
0.15	576.2	10.4	710.8	14.0	55.8	530.1
	2.0				2.7	1.8
0.20	576.2	10.4	710.8	14.0	55.8	530.1
	2.0				2.6	1.8
TeO_2	576.1	10.4				
	2.1					
Fe_2O_3			711.0	14.0	55.8	
			4.5		3.0	
FeO			709.5		54.7	
			4.5		3.0	

The uncertainty in the peak position is ±0.10 eV and in FWHM is ±0.20 eV.

spin–orbit doublet separation of 10.4 ± 0.2 eV as shown in Table 2. The Te $3d_{5/2}$ peaks are symmetric with a full-width at half-maximum (FWHM) varying between 2.0 and 2.3 eV. These values compare very favorable to those obtained on TeO_2 powder – 576.1 eV, 2.1 eV, and 10.4 eV for the BE, FWHM, and doublet separation, respectively.

3.2. O1s spectra

The O 1s spectra are displayed in Fig. 2 for all glass compositions. The O 1s peaks are very symmetric with FWHM ranging from 2.1 to 1.8 eV and are at approximately the same BE, 530.2 eV, for all four compositions, as shown in Table 2. Although fits to the O 1s spectra with two Gaussian–Lorentzian peaks were attempted, a single Gaussian–Lorentzian peak was found to result in the best fit indicating that the oxygen atoms in these glasses have a similar environment independent of the Fe_2O_3 content in the glass.

3.3. Fe2p spectra

The Fe 2p spin–orbit doublet core level spectra presented in Fig. 3 display a large background, which is typical for Fe 2p spectra and arises from inelastically scattered electrons. The Fe 2p peaks are fairly broad with the peak intensity increasing with increasing Fe_2O_3 content as expected. The BE of the Fe $2p_{3/2}$ is 710.8 eV for all glass compositions with an energy separation between the spin–orbit doublet of 14 eV. There is also a very small satellite structure at a binding energy of ~719 eV for the $x = 0.20$ composition, which is not apparent in the other glass compositions and may be hidden in the inelastic background of these glasses.

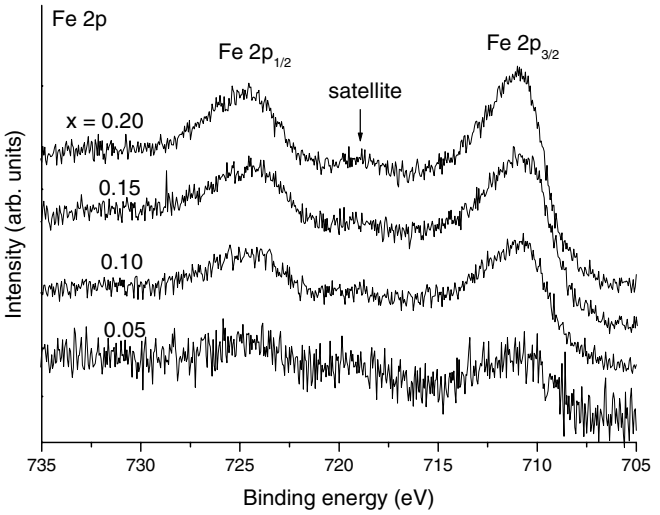

Fig. 3. Core level Fe 2p spectra for the $x(Fe_2O_3)$–$(1-x)(TeO_2)$ glasses.

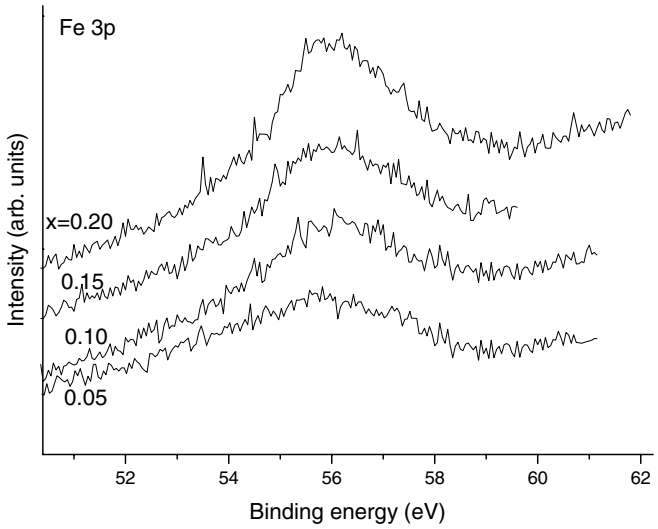

Fig. 4. Core level Fe 3p spectra for the $x(Fe_2O_3)$–$(1-x)(TeO_2)$ glasses.

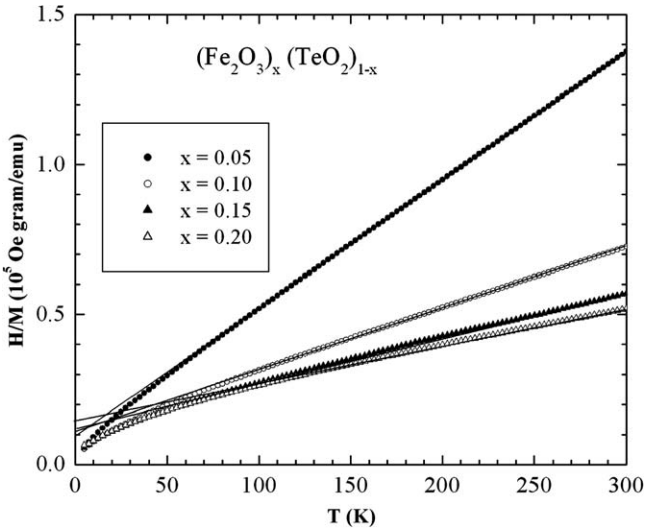

Fig. 6. The inverse of the magnetic susceptibility (H/M) as a function of temperature for the $x(Fe_2O_3)$–$(1-x)(TeO_2)$ glasses.

3.4. Fe 3p spectra

The Fe 3p spectra for the four glass compositions were also measured as the inelastic background is significantly smaller than for the Fe 2p spectra and there is no spin–orbit splitting of the Fe 3p peak. As seen in Fig. 4, the Fe 3p peak intensity increases with increasing Fe_2O_3 content while the peak position remains essentially unchanged at 56 eV. Although the Fe 3p peaks are fairly broad with a FWHM of ~3 eV, the FWHM are still significantly smaller than those for the Fe 2p spectra.

3.5. Temperature-dependent magnetization

The magnetic susceptibility results for these glasses are displayed in Fig. 5 as plots of the magnetic susceptibility, M/H, as a function of the temperature, T. The susceptibility data for all glass compositions follow a Curie–Weiss behavior ($M/H = C/(T-\theta)$) at temperatures greater than 100 K as shown in Fig. 6. The resulting parameters – the Curie constant C, the paramagnetic Curie temperature θ, and the effective magnetic moment p_{eff} – obtained from a least-squares fitting procedure are listed in Table 3 for all compositions.

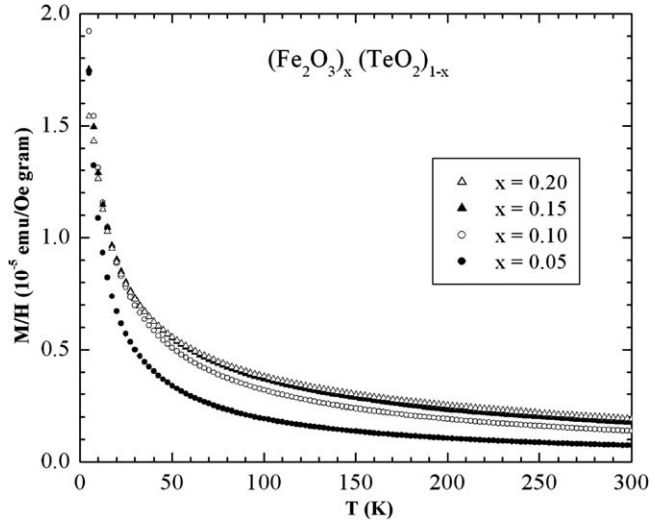

Fig. 5. Magnetic susceptibility versus temperature for the $x(Fe_2O_3)$–$(1-x)(TeO_2)$ glasses.

Table 3
Magnetic susceptibility results for $x(Fe_2O_3)$–$(1-x)(TeO_2)$ glasses

x		Curie constant $C\left(\frac{10^{-3}\text{ emu}}{\text{g Oe}}\right)$	θ (K)	p_{eff} (μ_B)
Batch	Actual			
0.05	0.043	2.33	−20.8	5.88
0.10	0.087	4.88	−54.5	5.98
0.15	0.13	6.98	−97.7	5.85
0.20	0.15	8.13	−123.0	5.98

4. Discussion

As seen from Table 2, the similarities in the values for the peak position, FWHM, and energy separation of the Te 3d core level spectra for all glass samples with those measured for the TeO_2 powder suggest that the Te ions exist in a similar environment, i.e., primarily in the TeO_4 tbp environment. In fact, the 3 eV difference between the Te $3d_{5/2}$ binding energies for Te atoms in a TeO_4 environment (~576 eV) [6] and in the TeO_3 tp environment (~573 eV) [15] is well within our XPS instrumental energy resolution (~1.0 eV) such that if TeO_3 structural units existed in these glass samples, their contribution should have been easily distinguishable from those of TeO_4. Moreover, the smaller FWHM of the Te $3d_{5/2}$ peaks in our Fe–Te glasses (~2.1 eV) compared to the FWHM measured in the Mo–Te glasses (~2.6 eV) infers the absence of TeO_{3+1}

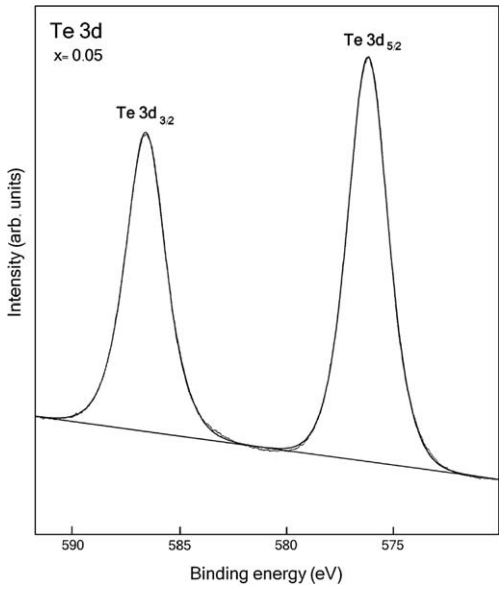

Fig. 7. The Te 3d spectrum for the $x = 0.05$ Fe_2O_3 tellurite glass sample and the resultant curve fitting to a single Gaussian–Lorentzian peak.

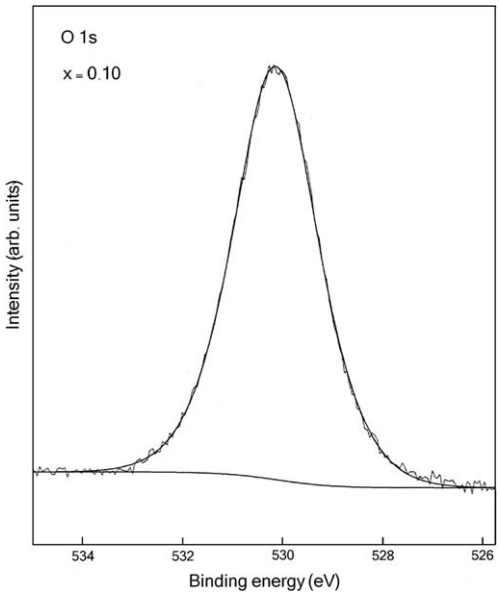

Fig. 8. The O 1s spectrum for the $x = 0.10$ Fe_2O_3 tellurite glass sample and the resultant curve fitting to a single Gaussian–Lorentzian peak.

structural units. Finally, curve fits of the Te $3d_{5/2}$ peak spectra with two contributions resulted in the convergence of the curves into a single contribution centered at 576 eV as shown in Fig. 7 for the $x = 0.05$ glass composition. These observations lead to the conclusion that the addition of Fe_2O_3 does not result in a change of the local TeO_2 structure from the basic TeO_4 trigonal bipyramid (tbp) structural units.

With the introduction of Fe_2O_3 into these tellurite glasses, the oxygen atoms can have three possible bond configurations, Te–O–Te, Te–O–Fe, and Fe–O–Fe. This leads to possible existence of non-bridging oxygen atoms (NBO), which should give rise to a shoulder on the lower BE side of the main O 1s peak and thus an asymmetry in the O 1s spectra. However, the O 1s spectra shown in Fig. 2 do not have any apparent asymmetry and the FWHM of ~2.0 eV are fairly narrow. Moreover, the O 1s spectra can be fitted with a single Gaussian–Lorentzian peak as shown in Fig. 8 for the $x = 0.10$ glass composition. Thus one concludes that all three configurations must have nearly the same BE in order for the O 1s peaks to be so symmetric. This absence of an asymmetry and NBO can be easily understood by the fact that Fe and Te atoms have similar electronegativities, 1.9 eV and 2.1 eV, respectively, and therefore have similar bond properties with the central oxygen atom.

It is well known that the core level spectrum of Fe(II)O has a $2p_{3/2}$ BE of ~709.6 eV with a weak and broad shake-up satellite at ~5 eV on its higher BE side [16]. In contrast the core level spectrum for Fe_2(III)O_3 has a $2p_{3/2}$ BE of ~711 eV and a satellite at ~8 eV on the higher BE side of the main peak [17]. Unfortunately, the high inelastic background and the broad nature of the Fe 2p spectra make it difficult to accurately curve fit the spectra into separate contributions from the Fe^{2+} and Fe^{3+} ions. In order to improve the reliability in determining the valence state of Fe ions in these tellurite glasses, the Fe 3p spectra for all glass samples have also been analyzed. Although the Fe 3p peaks appear to be symmetric with no apparent shoulder on either side of the main peak, the spectra were fitted to two contributions, one from the Fe^{2+} ions (~53.5 eV) and the other from the Fe^{3+} ions (~56 eV) [18]. For all four spectra, the fitting program converges to a single peak at ~56 eV with a FWHM of ~3 eV as shown in Fig. 9 for the $x = 0.10$ and 0.20 glass compositions. Thus the valence state of the Fe ions in these glasses is predominantly 3+ based on this analysis of the XPS measurements.

As described previously, the magnetic susceptibility data follow a Curie–Weiss-like temperature-dependent behavior, at least for temperatures above 100 K. From the Curie constant C in conjunction with the Fe concentration determined by chemical analysis on these oxide glasses, the effective magnetic moment, p_{eff}, varies from 5.85 μ_B to 5.98μ_B as shown in Table 3. These values are within 2% of the p_{eff} value of 5.9 μ_B for Fe^{3+} (compared to 5.4 μ_B for Fe^{2+}), which is well within the experimental uncertainty resulting from the Fe concentration and magnetization determinations. The negative paramagnetic Curie temperature values in the range of −20.7 to −123 K indicate a strong antiferromagnetic interaction between the Fe^{3+} ions. These large values are not surprising since θ is proportional to the number of neighboring magnetic ions (Fe–O–Fe) as well as the strength of the magnetic interaction. In fact, the downward trends of the H/M versus T curves in Fig. 6 are indicative of short-range antiferromagnetically ordered magnetic clusters beginning to behave as superparamagnetic particles.

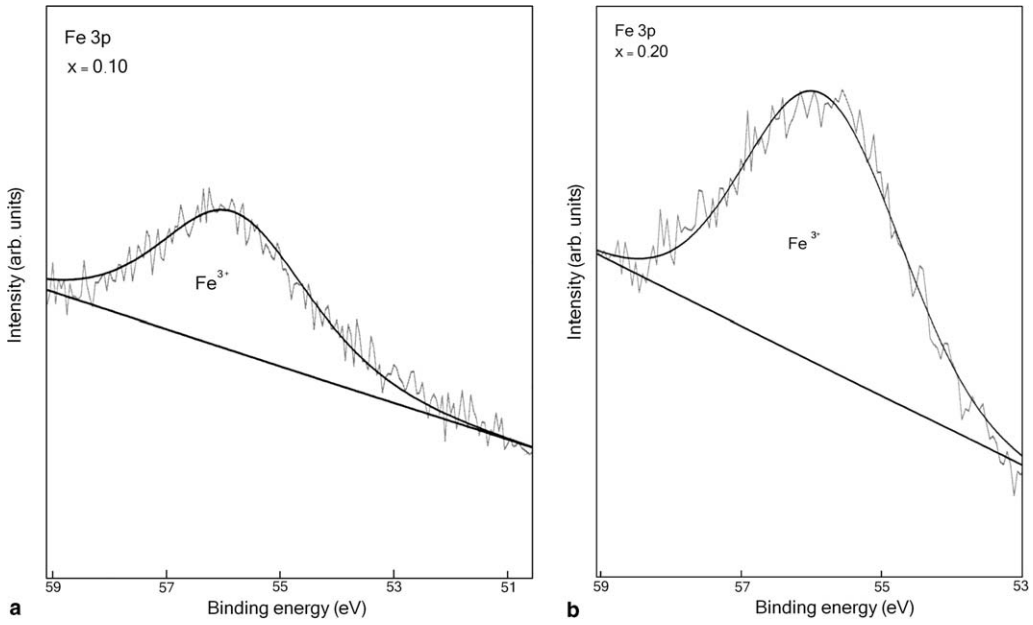

Fig. 9. The Fe 3p spectra for the (a) $x = 0.10$ and (b) 0.20 Fe_2O_3 tellurite glass samples and the resultant curve fitting to a single Gaussian–Lorentzian peak for Fe^{3+}.

5. Conclusion

XPS has been used to investigate the effect of increasing Fe_2O_3 content on the local structure of TeO_2 glasses. For Fe_2O_3 concentrations up to 20 mol%, the Te atoms appear to exist in a TeO_4 trigonal bipyramid (tbp) structural configuration with no TeO_3 trigonal pyramid (tp) units being detectable. Likewise, the strong similarity of all O 1s spectra indicates all three possible oxygen configurations, Te–O–Te, Te–O–Fe, and Fe–O–Fe, contribute to the same peak and consequently have very similar binding energies. The analysis of the Fe 3p spectra indicates that iron exists predominantly in the Fe^{3+} state which is consistent with the determinations from the magnetization measurements.

Acknowledgements

Two of the authors (A. Mekki and G.D. Khattak) would like to acknowledge the support of KFUPM. This work was supported by the Research Committee at KFUPM under Grant # SAB/2004/04.

References

[1] Y. Himei, Y. Miura, T. Nanba, A. Osaka, J. Non-Cryst. Solids 211 (1997) 64.
[2] R.A. El Mallawany, G.A. Saunders, J. Mater. Sci. Lett. 7 (1988) 870.
[3] Y. Himei, A. Osaka, T. Namba, Y. Miura, J. Non-Cryst. Solids 177 (1995) 164.
[4] Y. Dimitriev, V. Dimitrov, Mater. Res. Bull. 13 (1978) 1071.
[5] P. Charton, L. Gengember, P. Armand, J. Solid State Chem. 168 (2002) 175.
[6] G.D. Khattak, A. Mekki, L.E. Wenger, J. Non-Cryst. Solids 337 (2004) 174.
[7] A. Mekki, G.D. Khattak, L.E. Wenger, J. Non-Cryst. Solids 351 (2005) 2493.
[8] A. Mekki, G.D. Khattak, Phys. Chem. Glasses 46 (2005) 161.
[9] J. Heo, D. Lam, G.H. Sigel Jr., E.A. Mendoza, D.A. Hensley, J. Am. Ceram. Soc. 75 (1992) 277.
[10] T. Sekia, N. Machida, A. Ohtsuka, M. Tonokawa, J. Non-Cryst. Solids 144 (1992) 128.
[11] T. Yoko, M. Fujita, F. Miyaji, S. Sakka, Chem. Expr. 5 (1990) 549.
[12] H. Yamamamoto, H. Nasu, J. Katsuoka, K. Kamiya, J. Non-Cryst. Solids 170 (1994) 87.
[13] K. Suzuki, J. Non-Cryst. Solids 95&96 (1987) 15.
[14] R. Bruckner, H.U. Chun, H. Goretski, M. Sammet, J. Non-Cryst. Solids 42 (1980) 49.
[15] B.V.R. Chowdari, K.L. Tan, F. Ling, Solid State Ionics 113–118 (1998) 711.
[16] P. Mills, J.L. Sullivan, J. Phys. D 16 (1983) 723.
[17] H. Konno, M. Nagayama, J. Electron. Spectrosc. Relat. Phenom. 18 (1980) 341.
[18] A. Mekki, D. Holland, C.F. McConville, M. Salim, J. Non-Cryst. Solids 208 (1996) 267.